

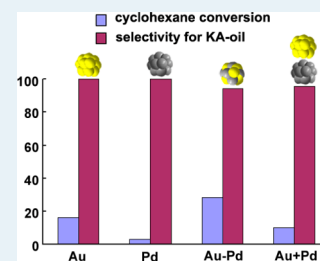
# Selective Oxidation of Saturated Hydrocarbons Using Au–Pd Alloy Nanoparticles Supported on Metal–Organic Frameworks

Jilan Long, Hongli Liu, Shijian Wu, Shijun Liao, and Yingwei Li\*

Key Laboratory of Fuel Cell Technology of Guangdong Province, School of Chemistry and Chemical Engineering, South China University of Technology, Guangzhou 510640, China

**ABSTRACT:** Gold (Au) and palladium (Pd) nanoparticles dispersed on a zeolite-type metal–organic framework (i.e., MIL-101) were prepared via a simple colloidal method. The catalysts were characterized by powder X-ray diffraction, N<sub>2</sub> physical adsorption, atomic absorption spectroscopy, transmission electron microscopy, energy-dispersive X-ray spectroscopy, and X-ray photoelectron spectroscopy. Au and Pd were mostly in the form of bimetallic alloys on the MIL-101 support. The Au–Pd/MIL-101 was active and selective in the oxidation of a variety of saturated (including primary, secondary, and tertiary) C–H bonds with molecular oxygen. For the liquid-phase oxidation of cyclohexane, cyclohexane conversion exceeding 40% was achieved (TOF: 19 000 h<sup>−1</sup>) with >80% selectivity to cyclohexanone and cyclohexanol under mild solvent-free conditions. Moreover, the Au–Pd alloy catalyst exhibited higher reactivity than their pure metal counterparts and an Au + Pd physical mixture. The high activity and selectivity of Au–Pd/MIL-101 in cyclohexane aerobic oxidation may be correlated to the synergistic alloying effect of bimetallic Au–Pd nanoparticles.

**KEYWORDS:** oxidation, saturated C–H bonds, metal–organic frameworks, gold, palladium, bimetallic catalysts



## 1. INTRODUCTION

Selective hydrocarbon oxidation is of academic as well as industrial significance for the production of valuable chemicals and intermediates, such as ketones and alcohols.<sup>1</sup> Among various oxidation transformations, selective oxidation of saturated hydrocarbons using environmentally benign molecular oxygen is believed to be one of the most problematic processes to control because of the inertness of saturated C–H bonds and the overoxidation issues derived from the increasing reactivity of products, as compared with starting materials. As an example, industrial production of cyclohexanone and cyclohexanol (also known as KA-oil) from cyclohexane oxidation using molecular oxygen as oxidant has to be carefully controlled (at conversions <5% with 75–80% selectivity for KA-oil) to avoid the formation of excessive amounts of byproducts owing to overoxidation.<sup>2–5</sup> As is well-known, cyclohexanone and cyclohexanol are important chemical intermediates for the bulk production of polyamide and plastics, such as Nylon 6 and Nylon 66.<sup>6</sup>

Currently, the commercial processes for the production of KA-oil from cyclohexane oxidation normally employ homogeneous transition-metal salts as catalysts, which have suffered from serious problems, such as corrosion and pollution. Therefore, over the past few decades, a great deal of research effort has been devoted to finding alternative and more environmentally sound methodologies to achieve a selective oxidation of cyclohexane. Heterogeneous catalysis can play a key role in the development of sustainable processes for these oxidation transformations, and a number of heterogeneous metal catalysts have been explored in this regard.<sup>7–27</sup> Among these heterogeneous catalyst systems, supported Au catalysts have received the most attention in recent years because of the unique selectivity in cyclohexane aerobic oxidation.<sup>7–15</sup> However, the attainment of high selectivities

(>80%) at elevated conversion (>30%) still remains a great challenge. More recently, carbon-based materials were attempted as metal-free catalysts for this transformation, but they also furnished a low yield of KA-oil in the liquid phase oxidation of cyclohexane.<sup>28,29</sup>

Metal–organic frameworks (MOFs) are a new class of hybrid porous materials assembled with metal cations and organic ligands.<sup>30</sup> Owing to their high surface area, porosity, and chemical tunability, the uses of MOFs as heterogeneous catalysts have recently received tremendous attention, especially for using MOFs as supports for metal (e.g., Pd, Au, Ru, and Pt) nanoparticles.<sup>31–44</sup> Very recently, MOF-supported Au nanoparticles have also been employed as catalysts for the aerobic oxidation of cyclohexane to cyclohexanone and cyclohexanol.<sup>15</sup>

It has been long known that metal alloying can promote catalytic activity or selectivity of the monometal species.<sup>45</sup> In recent years, Au–Pd bimetallic nanoparticles have attracted considerable interest owing to their high activities and selectivities in a number of oxidation reactions;<sup>43,46–50</sup> however, to the best of our knowledge, there is currently no report of using Au–Pd bimetallic nanoparticles as catalysts for the oxidation of cyclohexane. In this work, we report, for the first time, a highly active, selective, and reusable heterogeneous Au–Pd alloying catalyst, which was deposited on a zeolite-type MOF (i.e., MIL-101), in the liquid-phase aerobic oxidation of cyclohexane. It is shown that the synergy effect between Au and Pd leads to an enhanced performance of cyclohexane aerobic oxidation.

**Received:** November 22, 2012

**Revised:** January 21, 2013

**Published:** March 11, 2013

## 2. EXPERIMENTAL SECTION

**2.1. Chemicals.** All chemicals were purchased from commercial sources and used without further treatments. All solvents were analytical grade and distilled prior to use.

**2.2. Catalyst Preparation and Characterization.** MIL-101 was synthesized and purified according to the reported procedures.<sup>51</sup> MIL-101-supported Au–Pd catalysts were prepared by a sol–gel method. In a typical synthesis, an aqueous solution of HAuCl<sub>4</sub> and PdCl<sub>2</sub> ( $1 \times 10^{-3}$  M) was first prepared with PVP (polyvinylpyrrolidone) as a protecting agent (PVP monomer/(Au + Pd) = 10:1, molar ratio). The mixture was vigorously stirred for 1 h in an ice bath of 0 °C. Then a freshly prepared solution of NaBH<sub>4</sub> (0.1 M, NaBH<sub>4</sub>/(Au + Pd) = 5:1, molar ratio) was injected rapidly to the solution to obtain a dark brown sol. Within a few minutes of sol generation, the activated MIL-101 was added to the colloidal solution and stirred for 6 h, followed by washing thoroughly with deionized water. The sample was dried under vacuum at 100 °C for 2 h and then heated at 200 °C in H<sub>2</sub> for 2 h. The metal loadings (Au + Pd) for all the samples were around 1 wt %, on the basis of atomic absorption spectroscopy (AAS) analysis (Table 1).

**Table 1. Surface Areas, Pore Volumes, and Metal Loadings of the MIL-101 Samples**

sample	Au + Pd (wt%)	Au/Pd molar ratio	$S_{\text{BET}}$ (m <sup>2</sup> g <sup>-1</sup> )	$S_{\text{Langmuir}}$ (m <sup>2</sup> g <sup>-1</sup> )	$V_{\text{pore}}$ (cm <sup>3</sup> g <sup>-1</sup> )
MIL-101			3251	4494	1.60
Pd/MIL-101	1.03	0:1	3051	4397	1.55
Au/MIL-101	0.99	1:0	2974	4274	1.53
Au–Pd/MIL-101	0.97	1:1.9	2907	4202	1.49
Au–Pd/MIL-101	0.97	1:1.6	2887	4156	1.48
Au–Pd/MIL-101	1.05	1:1.4	2872	4108	1.48
Au–Pd/MIL-101	0.98	1:1	2500	3510	1.32
Au–Pd/MIL-101	0.99	1.4:1	2851	4076	1.47
Au–Pd/MIL-101	0.99	1.8:1	2767	3964	1.42
Au–Pd/MIL-101	0.97	2.6:1	2623	3761	1.36

Powder X-ray diffraction patterns of the samples were obtained on a Rigaku diffractometer (D/MAX-III A, 3 kW) using Cu K $\alpha$  radiation (40 kV, 30 mA, 0.1543 nm). BET surface area and pore size measurements were performed with N<sub>2</sub> adsorption/desorption isotherms at 77 K on a Micromeritics ASAP 2020 instrument. Before the analysis, the samples were degassed at 150 °C overnight. The metal loadings of the samples were measured quantitatively by atomic AAS on a Hitachi Z-2300 instrument. The size and morphology of the samples were investigated by using a transmission electron microscope (TEM, JEOL, JEM-2010HR) with energy-dispersive X-ray spectroscopy (EDS) analysis. Prior to analysis, solids were suspended in ethanol and deposited straight away on a copper grid. X-ray photoelectron spectroscopy (XPS) measurements were performed on a Kratos Axis Ultra DLD system with a base pressure of  $10^{-9}$  Torr. Infrared spectra were recorded on a Thermo Scientific Nicolet iS10 spectrometer use Smart OMNI-Transmission Accessory.

The metal dispersion was calculated by using the equation  $D_{\text{M}} = (6n_{\text{s}}M)/(\rho N d_{\text{p}})$ , where  $n_{\text{s}}$  is the number of atoms at the surface per unit area ( $1.15 \times 10^{19}$  m<sup>-2</sup> for Au, and  $1.06 \times 10^{19}$  m<sup>-2</sup> for Pd),  $M$  is the molecular weight (196.97 g mol<sup>-1</sup> for Au, and 106.42 g mol<sup>-1</sup> for Pd),  $\rho$  is the density (19.5 g cm<sup>-3</sup> for Au, and 12.02 g cm<sup>-3</sup> for Pd),  $N$  is  $6.023 \times 10^{23}$  mol<sup>-1</sup>, and  $d_{\text{p}}$  is the average particle size measured by HRTEM. The average

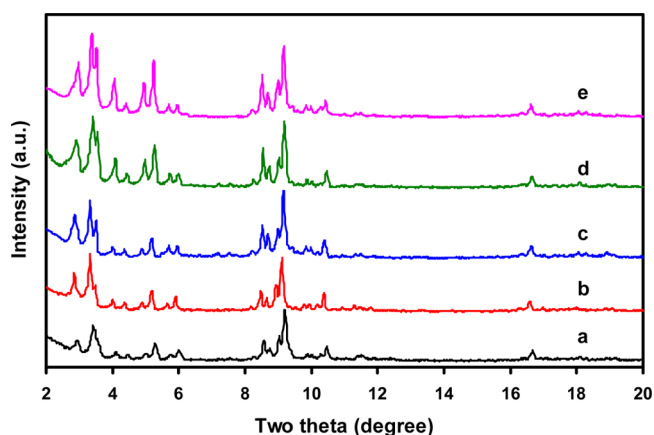
numbers of these parameters were used to calculate the metal dispersion considering the molar ratio of Au to Pd in the sample.

**2.3. Catalytic Testing.** The oxidation of cyclohexane was carried out in a 30 mL Parr batch reactor with a polytetrafluoroethylene (PTFE) liner. Typically, 10 mL of cyclohexane, 50 mg of solid catalyst, and anisole (as an internal standard) were added into the reactor. The autoclave was sealed and purged several times with pure O<sub>2</sub> to remove the air. Then the reactor was heated to 150 °C, and the O<sub>2</sub> pressure was adjusted to 1.0–1.5 MPa. After 4 h of reaction, the reactor was cooled to 0 °C. The gas phase composition was analyzed by a GC equipped with a TCD detector and a packed column (carbon molecular sieve TDX-01), which indicated that no gaseous product was produced in the reactions. The liquid products were analyzed using a GC (HP 6890 series) with a mass spectrometer detector (HP 5973 mass selective detector) and a capillary column (HP SMS).

For the recyclability test, after reaction, the Au–Pd/MIL-101 catalyst was separated from the reaction mixture by centrifugation, thoroughly washed with acetonitrile and ethyl acetate, dried at 80 °C, and then reused as catalyst for the next run.

## 3. RESULTS AND DISCUSSION

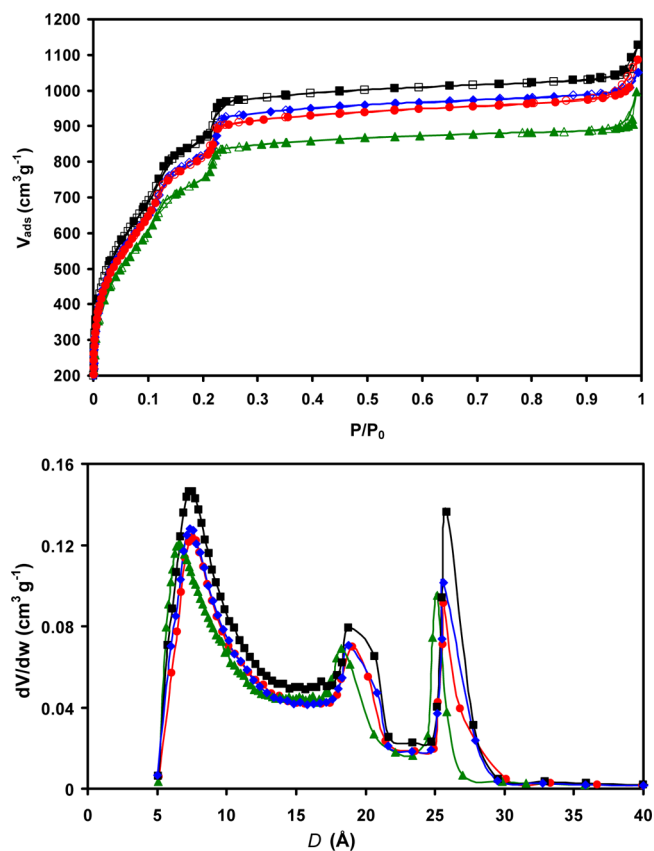
The powder XRD patterns (Figure 1) of the Au–Pd/MIL-101 samples all match with those of the parent MIL-101, indicating



**Figure 1.** Powder XRD patterns of MIL-101 samples: (a) MIL-101 (as-synthesized); (b) Au/MIL-101; (c) Pd/MIL-101; and Au–Pd/MIL-101 (Au/Pd molar ratio = 1.4:1) (d) before and (e) after catalytic reaction.

that the structure of MIL-101 was mostly maintained by using the developed preparation recipes. The stability of the porous structure of MIL-101 after metal doping could be further confirmed by the N<sub>2</sub> adsorption results at 77 K (Figure 2 and Table 1). The appreciable decrease in N<sub>2</sub> adsorption amount can be attributed to the blockage of cavities of MIL-101 by the metal nanoparticles located in the pore or at the surface of the MIL-101 framework. As evident from the pore size distribution curves (Figure 2), the introduction of metal leads to a slight decrease in the pore sizes of MIL-101. The window diameters of the two large cages of MIL-101 are reported to be  $\sim 12$  and  $16$  Å respectively,<sup>51</sup> which make the cages accessible to very large molecules.

TEM characterization revealed that the Au–Pd nanoparticles were homogeneously dispersed in the materials, with particle sizes typically between 2 and 3 nm (average size:  $2.40 \pm 0.63$  nm) (Figure 3). No significant formation of aggregates was observed.

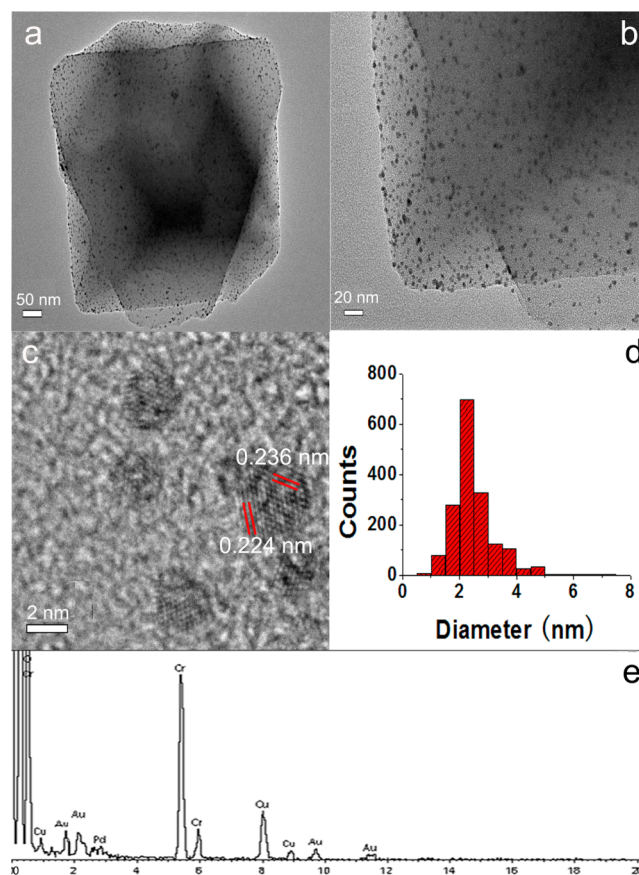


**Figure 2.** Nitrogen adsorption/desorption isotherms at 77 K (top) and Horvath–Kawazoe pore-size distribution curves (bottom) of the as-synthesized MIL-101 (■), Pd/MIL-101 (◆), Au/MIL-101 (●), and Au–Pd/MIL-101 (Au/Pd = 1.4:1) (▲).

The high-resolution images of Au–Pd/MIL-101 (Figure 3c) showed that the particles were highly faceted and twinned in character. The interplanar spacings of the particle lattice were 0.224 or 0.236 nm, which agree well with the (111) lattice spacing of face-centered cubic Pd and cubic Au, respectively. The TEM results indicated that Au and Pd formed mostly bimetallic alloys on the MIL-101 support by using the present deposition method. The metal dispersion was calculated to be  $\sim 49\%$ , on the basis of the average particle size of Au–Pd, assuming spherical particles.

XPS data indicated that the Au(0) 4f and Pd(0) 3d peaks for the Au–Pd/MIL-101 (Au/Pd molar ratio = 1.4:1) were shifted to lower binding energies by  $\sim 0.4$  and  $0.3$  eV, respectively, with respect to the monometallic Au/MIL-101 and Pd/MIL-101 samples (Figure 4). Such an observed negative shift for both Au 4f and Pd 3d binding energies was previously reported and reflected a modification of the electronic structure of the surface Au and Pd atoms, which could be indicative of the formation of Au–Pd bimetallic alloys.<sup>50,52</sup> In Au–Pd alloy, Pd is generally more electronegative and gains d electrons from Au, which is supposed to be compensated by the depletion of core s or p electron count (i.e., net charge flowing into Au).<sup>53,54</sup>

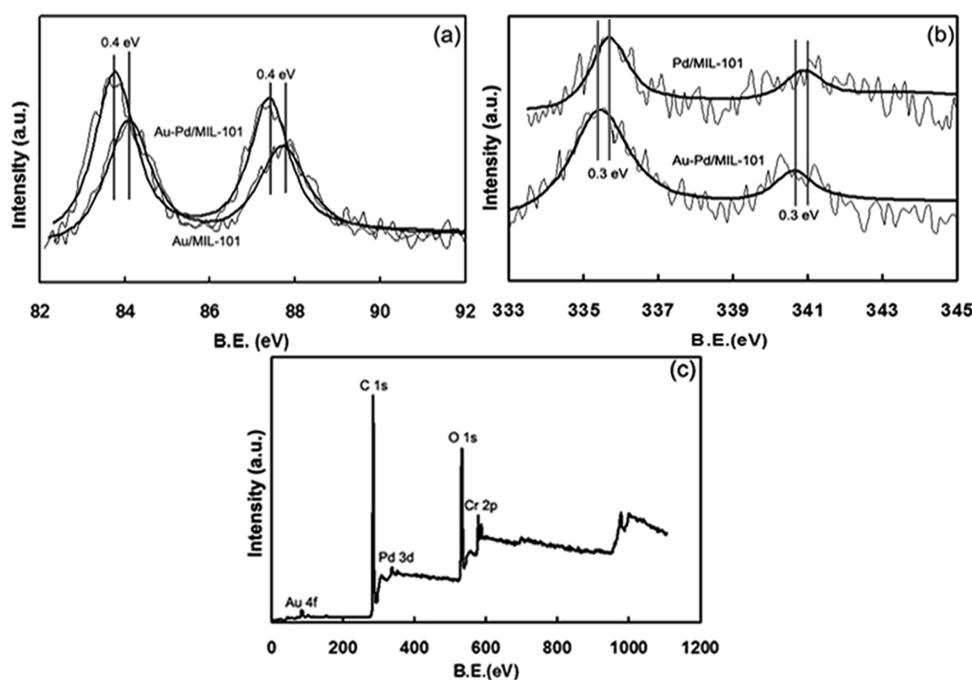
The solvent-free oxidation of cyclohexane was carried out at  $150$  °C and  $1.0$  MPa of  $\text{O}_2$ . Blank runs gave essentially no activity in the systems (even with the parent MIL-101) after 4 h of reaction (Table 2, entries 1 and 2). The introduction of a small amount of Au onto MIL-101 remarkably improved the conversion of cyclohexane with  $>99.9\%$  selectivity for KA-oil (Table 2, entry 3). Interestingly, the activity could be further



**Figure 3.** (a–c) TEM images of Au–Pd/MIL-101 (Au/Pd molar ratio = 1.4:1), (d) corresponding size distribution of Au–Pd nanoparticles, and (e) the EDS pattern.

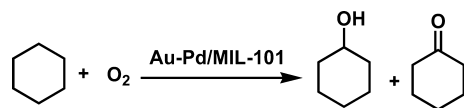
improved with the addition of Pd, and the Au–Pd/MIL-101 catalysts with different Au/Pd ratios were subsequently screened in the aerobic oxidation of cyclohexane (Table 2, entries 4–11). The results of the cyclohexane oxidation pointed to an optimized performance of Au–Pd/MIL-101 with a 1.4:1 Au/Pd molar ratio (Table 2, entry 6), which provided the highest KA-oil yield and TOF value with a high selectivity for KA-oil ( $\sim 95\%$ ). Further increasing the content of Pd in the catalysts resulted in lower conversions and yields of KA-oil (Table 2, entries 7–11). The use of monometallic Pd/MIL-101 as catalyst gave a very low conversion of cyclohexane under the investigated conditions (Table 2, entry 11). We also examined the reactivity of the physical mixture of pure Au and Pd catalysts (Au/Pd molar ratio = 1.4:1). The physical mixture exhibited a much lower activity as compared with the bimetallic alloying Au–Pd/MIL-101 catalyst under identical conditions (Table 2, entries 6 and 12). These results demonstrated a clear synergistic effect for the Au–Pd alloying catalysts, as compared with the monometallic Au or Pd species.

Using the optimized Au–Pd catalyst, a further optimization of the reaction parameters was subsequently conducted. The  $\text{O}_2$  pressure and reaction temperature were found to strongly influence the reaction. The conversion of cyclohexane was remarkably enhanced with increasing the pressure and temperature (Table 2, entries 6, 13, and 14). Nevertheless, an increase in pressure and temperature also led to a decrease in the selectivity to KA-oil. This reduction in selectivity was attributed to the enhanced overoxidation of cyclohexanol and cyclohexanone at elevated temperatures or pressures over the Au–Pd catalyst.



**Figure 4.** XPS spectra of Au/MIL-101, Pd/MIL-101, and Au–Pd/MIL-101 (Au/Pd molar ratio = 1.4:1): (a) Au 4f, (b) Pd 3d, and (c) survey spectra of Au–Pd/MIL-101.

**Table 2. Results of the Oxidation of Cyclohexane in the Absence of Solvent<sup>a</sup>**



entry	Au/Pd molar ratio	concn (%)	sel (%) <sup>b</sup>		yield of KA-oil (%)
			OH	C=O	
1 <sup>c</sup>		trace			
2 <sup>d</sup>		<2.0	36.1	52.9	<2.0
3	1:0	16.2	18.2	81.8	16.2
4	2.6:1	16.5	19.0	80.6	16.5
5	1.8:1	20.0	15.8	81.0	19.4
6	1.4:1	28.4	16.1	78.3	26.8
7	1:1	21.3	9.8	80.8	19.3
8	1:1.4	10.4	7.7	92.3	10.4
9	1:1.6	9.4	5.5	93.8	9.3
10	1:1.9	4.2		>99.9	4.2
11	0:1	<3.0		>99.9	<3.0
12 <sup>e</sup>	1.4:1	10.0	17.0	78.6	9.6
13 <sup>f</sup>	1.4:1	45.4	27.2	57.0	38.2
14 <sup>f,g</sup>	1.4:1	50.8	27.7	50.2	39.6
15 <sup>f,h</sup>	1.4:1	41.5	31.3	53.1	35.0
16 <sup>f,h,i</sup>	1.4:1	37.6	28.7	55.3	31.6
17 <sup>j</sup>	1.4:1	2.3		19.0	0.4

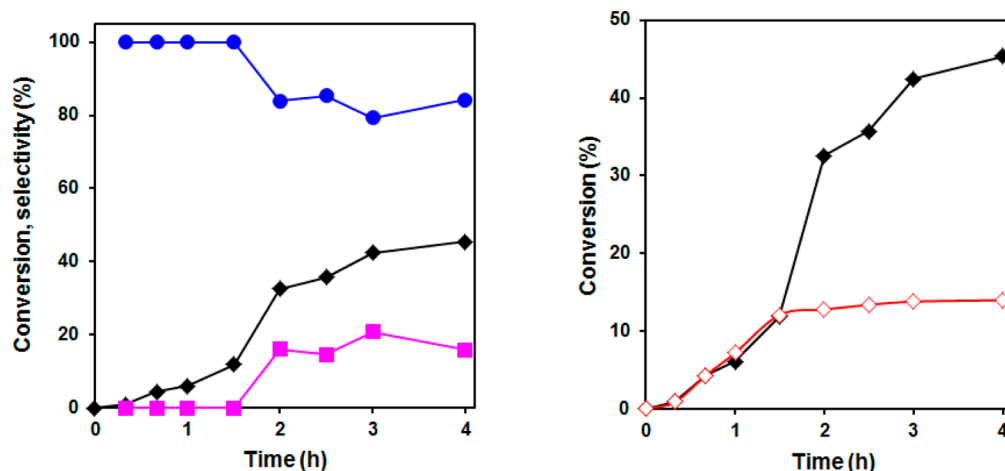
<sup>a</sup>Reaction conditions: cyclohexane (10 mL), catalyst (50 mg), O<sub>2</sub> (1.0 MPa), 150 °C, 4 h. <sup>b</sup>C=O indicates cyclohexanone, and OH denotes cyclohexanol. Main byproducts: organic acids (e.g., adipic acid), formic acid cyclohexyl ester, and cyclohexyl hydroperoxide. <sup>c</sup>No catalyst used. <sup>d</sup>Catalyst: MIL-101. <sup>e</sup>Au/MIL-101 and Pd/MIL-101 physical mixture. <sup>f</sup>1.5 MPa of O<sub>2</sub>. <sup>g</sup>160 °C. <sup>h</sup>20 mL cyclohexane. <sup>i</sup>t = 2 h. <sup>j</sup>*p*-Benzoquinone (1 wt %) was added.

Under 150 °C and 1.5 MPa of O<sub>2</sub>, we investigated the oxidation of cyclohexane at a higher substrate/metal molar ratio

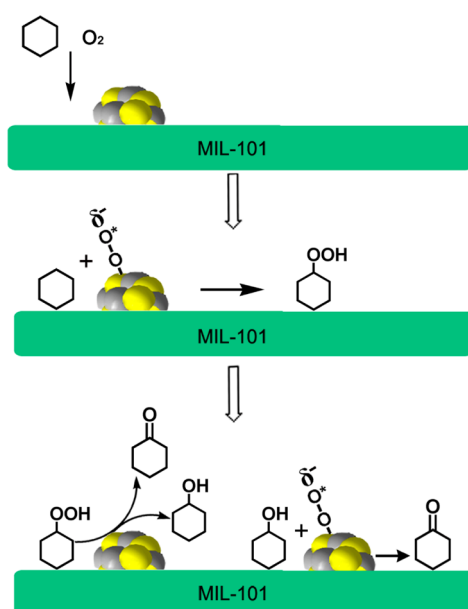
(0.0017 mol % Au + Pd). The reaction also proceeded smoothly, furnishing a conversion of 41.5% with a good selectivity (~85%) to KA-oil after 4 h of reaction (Table 2, entry 15). The turnover frequency (TOF: moles of KA-oil produced on per mole of surface Au–Pd per hour) was calculated to be ~19 000 h<sup>-1</sup> at 2 h of reaction (Table 2, entry 16), which is comparable to the highest TOF values reported to date on liquid-phase cyclohexane aerobic oxidation under similar reaction conditions.<sup>13</sup>

The reaction profile over an initial 4 h reaction period clearly showed an initiation period of ~20 min in which almost no conversion was observed (Figure 5). The presence of such an induction time was also observed in previous studies on liquid-phase cyclohexane oxidation.<sup>7</sup> It is widely suggested that the liquid-phase aerobic oxidation of cyclohexane involves radical intermediates, and the product cyclohexanone could also catalyze the initiation of the autoxidation process.<sup>28</sup> To test the possible involvement of radical species in our system, we added a radical scavenger (i.e., *p*-benzoquinone) to the reaction solution under the standard conditions. The reaction was almost fully suppressed to give a conversion of ~2.3% after 4 h of reaction (Table 2, entry 17). This result strongly suggests the involvement of radical species in the present reaction system.

In view of these findings, we have proposed a possible reaction pathway for the liquid-phase aerobic oxidation of cyclohexane into cyclohexanol and cyclohexanone over the Au–Pd/MIL-101 catalysts (Figure 6). Au nanoparticles have been widely reported as efficient catalysts for a variety of aerobic oxidation reactions, and the activation of O<sub>2</sub> could be promoted over Au clusters with a high electron density.<sup>55,56</sup> Therefore, the enhanced surface electron density of the bimetallic Au–Pd alloying catalyst as compared with monometallic Au (see XPS data) would be favorable for O<sub>2</sub> adsorption and activation to form active oxygen species, which is probably in a superoxo-like form (•O<sub>2</sub><sup>-</sup>).<sup>38,55–57</sup> Subsequently, the as-formed •O<sub>2</sub><sup>-</sup> reacts with adsorbed cyclohexane to produce the intermediate cyclohexyl hydroperoxide (CHHP) (Figure 6).<sup>29</sup> CHHP could be considered



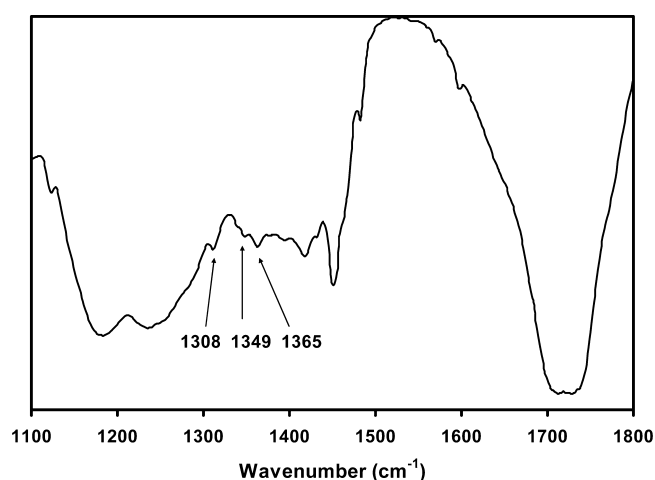
**Figure 5.** Cyclohexane conversion and product selectivity as a function of time: cyclohexane (10 mL), catalyst (50 mg), O<sub>2</sub> (1.5 MPa), 150 °C. Symbols: ◆, conversion; ●, selectivity to KA-oil; ■, selectivity to byproducts; ◇, cyclohexane conversion after removing the catalyst at 1.5 h.



**Figure 6.** Schematic representation of the mechanism for cyclohexane aerobic oxidation over Au–Pd/MIL-101.

as the first oxygenated product in this reaction,<sup>58,59</sup> which has been detected in cyclohexane aerobic oxidation by using in situ FT-IR characterization.<sup>60,61</sup> The presence of such a species in our system was also confirmed by FT-IR (Figure 7) as well as GC/MS analysis (Table 2). The IR spectrum of the reaction mixture after reaction showed three peaks at 1308, 1349, and 1365 cm<sup>-1</sup>, respectively, that can be assigned to the vibrational modes of cyclohexyl hydroperoxide.<sup>60,61</sup>

The formed CHHP then undergoes decomposition to produce cyclohexanone and cyclohexanol products. It is noteworthy that the ratios of cyclohexanone to cyclohexanol in the products of the Au–Pd catalyst system were all higher than 2:1 (Table 2), suggesting a possible catalytic mechanism of CHHP conversion to KA-oil over the Au–Pd catalysts, because a noncatalytic decomposition of CHHP generally results in a much lower ratio of cyclohexanone to cyclohexanol.<sup>1,7,28</sup> Moreover, the formed cyclohexanol could be further oxidized to cyclohexanone over the Au–Pd catalysts, leading to higher selectivity of cyclohexanone than cyclohexanol. Our previous results have demonstrated that




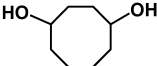
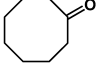
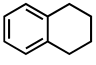
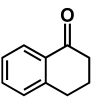
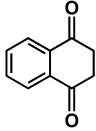
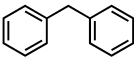
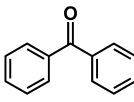
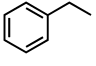
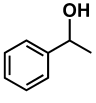
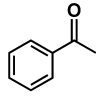

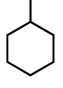
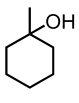
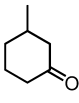
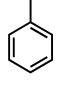
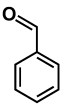
**Figure 7.** IR spectrum of the solution after 4 h of reaction of cyclohexane with oxygen using Au–Pd/MIL-101 as catalyst. The peaks at 1365, 1349, and 1308 cm<sup>-1</sup> can be assigned to the vibrational modes of cyclohexyl hydroperoxide.

MIL-101-supported Au or Pd nanoparticles were highly active and selective for the aerobic oxidation of cyclohexanol to cyclohexanone under mild conditions.<sup>38,62</sup>

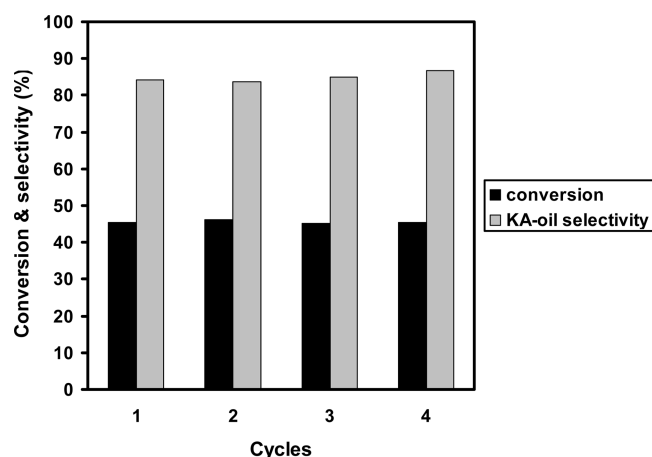
To demonstrate the general applicability of the Au–Pd/MIL-101 catalyst, we examined the efficacy of oxidation transformations of a variety of saturated alkanes under similar reaction conditions. Various secondary C–H bonds were oxidized smoothly with excellent selectivities to their corresponding oxidation products at moderate conversions (Table 3, entries 1–4). Under the standard conditions, Au–Pd/MIL-101 gave only a trace of conversion of *n*-hexane (Table 3, entry 5). This could be due to the weak adsorption of *n*-hexane on the catalyst, as also suggested in the literature reports.<sup>29</sup> Tertiary C–H bonds could also be oxidized to corresponding alcohols (Table 3, entry 6). It is interesting to note that Au–Pd/MIL-101 was also active in the oxidation of primary C–H bonds (e.g., toluene) with >95% selectivity to benzaldehyde (Table 3, entry 7), further confirming the wider applicability of our catalysts for the selective oxidation of saturated C–H bonds.

In a final set of experiments, we investigated the reusability of the Au–Pd catalyst because it is of importance to confirm that the highly active catalyst is stable and can be reused. After the

Table 3. Aerobic Oxidation of Various Alkanes Using Au–Pd/MIL-101<sup>b</sup>

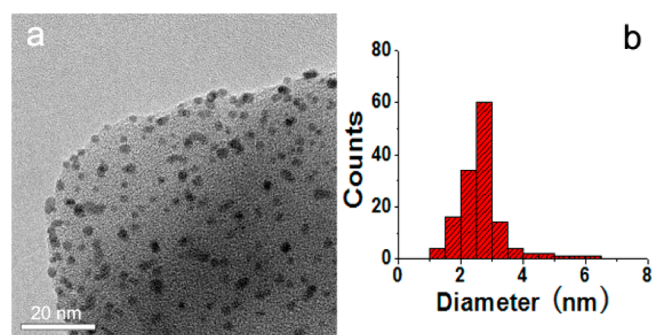
Entry	Substrate	Con. (%)	Sel. (%)	
1		51.8	 58.2	 22.6
2		34.5	 56.1	 38.1
3 <sup>a</sup>		19.4	 94.8	
4		38.5	 21.9	 65.3
5		trace		
6 <sup>a</sup>		32.3	 68.5	 13.2
7 <sup>a</sup>		4.0	 95.2	

<sup>a</sup>CH<sub>3</sub>CN (5 mL). <sup>b</sup>Reaction conditions: Substrate/metal = 10 000:1 (molar ratio), Au–Pd/MIL-101 (1.4:1 Au/Pd molar ratio), 50 mg, 150 °C, 1.5 MPa of O<sub>2</sub>, 4 h.



**Figure 8.** Reuses of the Au–Pd/MIL-101 catalyst in the liquid-phase oxidation of cyclohexane. Reaction conditions: cyclohexane (10 mL), Au–Pd/MIL-101 (1.4:1 Au/Pd molar ratio, 50 mg), O<sub>2</sub> (1.5 MPa), 150 °C, 4 h.

cyclohexane oxidation reaction, Au–Pd/MIL-101 (Au/Pd = 1.4:1) was separated from the reaction mixture by centrifugation, thoroughly washed with acetonitrile and ethyl acetate, dried at 80 °C, and then reused as the catalyst in subsequent runs under identical reaction conditions. Results included in Figure 8 reveal



**Figure 9.** TEM image (a) of Au–Pd/MIL-101 (Au/Pd molar ratio = 1.4:1) after catalytic reaction and (b) the corresponding size distribution of Au–Pd nanoparticles.

that no appreciable loss of conversion and selectivity was observed in the oxidation of cyclohexane up to four runs. Powder XRD characterization showed that the crystalline structure of MIL-101 was mostly retained (Figure 1). AAS experiments on the reaction mixtures indicated that only traces of metal (<1% of the total gold or palladium) was detected to have leached into the liquid phase during reaction. Moreover, the reaction after removing the catalyst from the solution at 1.5 h essentially stopped, strongly suggesting that the reaction proceeded mostly on the heterogeneous surface (Figure 5). TEM images of the

catalyst after the fourth run revealed a minimum aggregation of particles (average size:  $2.59 \pm 0.51$  nm) in the material (Figure 9). These results demonstrated that the highly active Au–Pd/MIL-101 catalyst was stable and reusable under the investigated conditions.

#### 4. CONCLUSIONS

In conclusion, we have developed a highly efficient heterogeneous catalyst system for liquid-phase aerobic oxidation of a variety of saturated hydrocarbons using MIL-101-supported Au–Pd nanoparticles as catalyst without the addition of any promoters. The Au–Pd bimetallic catalysts exhibited a marked superiority over their pure metal counterparts and a Au + Pd physical mixture in terms of cyclohexane conversion, suggesting a strong molecular-scale synergy of Au–Pd alloys. Radical intermediates were demonstrated to likely be involved in these transformations. Moreover, the Au–Pd catalyst was highly stabilized against metal agglomeration and leaching, maintaining the high activity and selectivity during a number of recycles under the investigated conditions. The combination of high activity and selectivity as well as good stability enables Au–Pd/MIL-101 a potential material for practical applications in liquid-phase aerobic oxidation of cyclohexane to cyclohexanone and cyclohexanol. Work is underway to investigate the reaction mechanism and further improve and optimize the catalytic system in our laboratories.

#### AUTHOR INFORMATION

##### Corresponding Author

\*E-mail: liyw@scut.edu.cn.

##### Notes

The authors declare no competing financial interest.

#### ACKNOWLEDGMENTS

This work was supported by the NSF of China (20936001 and 21073065), the NSF of Guangdong (S2011020002397 and 10351064101000000), the Doctoral Fund of Ministry of Education of China (20120172110012), and the Fundamental Research Funds for the Central Universities (2011ZG0009).

#### REFERENCES

- (1) Sheldon, R. A.; Kochi, J. K. *Metal-Catalyzed Oxidations of Organic Compounds*; Academic Press: New York, 1981.
- (2) Kamata, K.; Yonehara, K.; Nakagawa, Y.; Uehara, K.; Mizuno, N. *Nat. Chem.* **2010**, *2*, 478.
- (3) Bergman, R. G. *Nature* **2007**, *446*, 391.
- (4) Bartholomé, E. Cyclohexanol and cyclohexanone. In *Ullmanns Encyklopädie der Technischen Chemie*; Verlag Chemie: Weinheim, 1972, Vol. 4.
- (5) Weissmehl, K.; Horpe, H. J. *Industrial Organic Chemistry*, 2nd ed.; VCH Press: Weinheim, 1993.
- (6) Schuchardt, U.; Calvarlho, W. A.; Spinace, E. V. *Synlett* **1993**, *10*, 713.
- (7) Hereijgers, B. P. C.; Weckhuysen, B. M. J. *Catal.* **2010**, *270*, 16.
- (8) Zhao, R.; Ji, D.; Lv, G.; Qian, G.; Yan, L.; Wang, X.; Suo, J. *Chem. Commun.* **2004**, 904.
- (9) Lü, G.; Zhao, R.; Qian, G.; Qi, Y.; Wang, X.; Suo, J. *Catal. Lett.* **2004**, *97*, 115.
- (10) Xu, L.-X.; He, C.-H.; Zhu, M.-Q.; Fang, S. *Catal. Lett.* **2007**, *114*, 202.
- (11) Xu, L.-X.; He, C.-H.; Zhu, M.-Q.; Wu, K.-J.; Lai, Y.-L. *Catal. Commun.* **2008**, *9*, 816.
- (12) Wu, P.; Bai, P.; Loh, K. P.; Zhao, X. S. *Catal. Today* **2010**, *158*, 220.
- (13) Wu, P.; Bai, P.; Lei, Z.; Loh, K. P.; Zhao, X. S. *Microporous Mesoporous Mater.* **2011**, *141*, 222.
- (14) Li, L.; Jin, C.; Wang, X.; Ji, W.; Pan, Y.; Knaap, T. V. D.; Stoel, R. V. D.; Au, C. T. *Catal. Lett.* **2009**, *129*, 303.
- (15) Sun, Z.; Li, G.; Liu, L.; Liu, H. *Catal. Commun.* **2012**, *27*, 200.
- (16) Li, J.; Shi, Y.; Xu, L.; Lu, G. *Ind. Eng. Chem. Res.* **2010**, *49*, 5392.
- (17) Raja, R.; Sankar, G.; Thomas, J. M. J. *Am. Chem. Soc.* **1999**, *121*, 11926.
- (18) Reddy, S. S.; Raju, B. D.; Padmasri, A. H.; Sai Prakash, P. K.; Rama Rao, K. S. *Catal. Today* **2009**, *141*, 61.
- (19) Chen, C.; Xu, J.; Zhang, Q.; Ma, Y.; Zhou, L.; Wang, M. *Chem. Commun.* **2011**, *47*, 1336.
- (20) Yuan, H.-X.; Xia, Q.-H.; Zhan, H.-J.; Lu, X.-H.; Su, K.-X. *Appl. Catal., A* **2006**, *304*, 178.
- (21) Guo, X.; Shen, D.-H.; Li, Y.-Y.; Tian, M.; Liu, Q.; Guo, C.-C.; Liu, Z.-G. *J. Mol. Catal. A: Chem.* **2011**, *351*, 174.
- (22) Qian, G.; Ji, D.; Lu, G.; Zhao, R.; Qi, Y.; Suo, J. J. *Catal.* **2005**, *232*, 378.
- (23) Wang, H.; Li, R.; Zheng, Y.; Chen, H.; Wang, F.; Ma, J. *Catal. Lett.* **2008**, *122*, 330.
- (24) Yang, X.; Yu, H.; Peng, F.; Wang, H. *ChemSusChem* **2012**, *7*, 1213.
- (25) Gu, J.; Huang, Y.; Elangovan, S. P.; Li, Y.; Zhao, W.; Toshio, I.; Yamazaki, Y.; Shi, J. *J. Phys. Chem. C* **2011**, *115*, 21211.
- (26) Zhao, H.; Zhou, J.; Luo, H.; Zeng, C.; Li, D.; Liu, Y. *Catal. Lett.* **2006**, *108*, 49.
- (27) Zhao, R.; Wang, Y.; Guo, Y.; Guo, Y.; Liu, X.; Zhang, Z.; Wang, Y.; Zhan, W.; Lu, G. *Green Chem.* **2006**, *8*, 459.
- (28) Yu, H.; Peng, F.; Tan, J.; Hu, X.; Wang, H.; Yang, J.; Zheng, W. *Angew. Chem., Int. Ed.* **2011**, *50*, 3978.
- (29) Li, X. H.; Chen, J. S.; Wang, X.; Sun, J.; Antonietti, M. *J. Am. Chem. Soc.* **2011**, *133*, 8074.
- (30) Long, J. R.; Yaghi, O. M. *Chem. Soc. Rev.* **2009**, *38*, 1213.
- (31) Farrusseng, D.; Aguado, S.; Pinel, C. *Angew. Chem., Int. Ed.* **2009**, *48*, 7502.
- (32) Yuan, B. Z.; Pan, Y. Y.; Li, Y. W.; Yin, B. L.; Jiang, H. F. *Angew. Chem., Int. Ed.* **2010**, *49*, 4054.
- (33) Pan, Y. Y.; Yuan, B. Z.; Li, Y. W.; He, D. H. *Chem. Commun.* **2010**, *46*, 2280.
- (34) Zhao, Y.; Zhang, J.; Song, J.; Li, J.; Liu, J.; Wu, T.; Zhang, P.; Han, B. *Green Chem.* **2011**, *13*, 2078.
- (35) El-Shall, M. S.; Abdelsayed, V.; Khder, A. S.; Hassan, H. A.; El-Kaderi, H. M.; Reich, T. E. *J. Mater. Chem.* **2009**, *19*, 7625.
- (36) Li, H.; Zhu, Z.; Zhang, F.; Xie, S.; Li, H.; Li, P.; Zhou, X. *ACS Catal.* **2011**, *1*, 1604.
- (37) Cheon, Y. E.; Suh, M. P. *Angew. Chem., Int. Ed.* **2009**, *48*, 2899.
- (38) Liu, H. L.; Liu, Y. L.; Li, Y. W.; Tang, Z. Y.; Jiang, H. F. *J. Phys. Chem. C* **2010**, *114*, 13362.
- (39) Jiang, H. L.; Akita, T.; Ishida, T.; Haruta, M.; Xu, Q. *J. Am. Chem. Soc.* **2011**, *133*, 1304.
- (40) Jiang, H.; Liu, B.; Akita, T.; Haruta, M.; Sakurai, H.; Xu, Q. *J. Am. Chem. Soc.* **2009**, *131*, 11302.
- (41) Schröder, F.; Esken, D.; Cokoja, M.; van den Berg, M. W. E.; Lebedev, O. I.; Van Tendeloo, G.; Walaszek, B.; Buntkowsky, G.; Limbach, H. H.; Chaudret, B.; Fischer, R. A. *J. Am. Chem. Soc.* **2008**, *130*, 6119.
- (42) Park, Y. K.; Choi, S. B.; Nam, H. J.; Jung, D. Y.; Ahn, H. C.; Choi, K.; Furukawad, H.; Kim, J. *Chem. Commun.* **2010**, *46*, 3086.
- (43) Liu, H.; Li, Y. W.; Jiang, H.; Vargas, C.; Luque, R. *Chem. Commun.* **2012**, *48*, 8431.
- (44) Dhakshinamoorthy, A.; Alvaro, M.; Garcia, H. *Catal. Sci. Technol.* **2011**, *1*, 856.
- (45) Ponec, V.; Bond, G. C. *Catalysis by Metals and Alloys; Studies in Surface Science and Catalysis*; Elsevier: Amsterdam, 1995.
- (46) Balcha, T.; Strobl, J. R.; Fowler, C.; Dash, P.; Scott, R. W. J. *ACS Catal.* **2011**, *1*, 425.
- (47) Wang, D.; Villa, A.; Porta, F.; Su, D.; Prati, L. *Chem. Commun.* **2006**, 1956.
- (48) Kesavan, L.; Tiruvalam, R.; Ab Rahim, M. H.; bin Saiman, M. I.; Enache, D. I.; Jenkins, R. L.; Dimitratos, N.; Lopez-Sanchez, J. A.;

- Taylor, S. H.; Knight, D. W.; Kiely, C. J.; Hutchings, G. J. *Science* **2011**, *331*, 195.
- (49) Hermans, S.; Deffernez, A.; Devillers, M. *Catal. Today* **2010**, *157*, 77.
- (50) Liu, H.; Chen, G.; Jiang, H. F.; Li, Y. W.; Luque, R. *ChemSusChem* **2012**, *5*, 1892.
- (51) Férey, G.; Mellot-Draznieks, C.; Serre, C.; Millange, F.; Dutour, J.; Surblé, S.; Margiolaki, I. *Science* **2005**, *309*, 2040.
- (52) Xu, J.; White, T.; Li, P.; He, C.; Yu, J.; Yuan, W.; Han, Y. F. *J. Am. Chem. Soc.* **2010**, *132*, 10398.
- (53) Chou, T. S.; Perlman, M. L.; Watson, R. E. *Phys. Rev. B* **1976**, *14*, 3248.
- (54) Nascente, P. A. P.; de Castro, S. G. C.; Landers, R.; Kleiman, G. G. *Phys. Rev. B* **1991**, *43*, 4659.
- (55) Chowdhury, B.; Bravo-Suárez, J. J.; Mimura, N.; Lu, J.; Bando, K. K.; Tsubota, S.; Haruta, M. *J. Phys. Chem. B* **2006**, *110*, 22995.
- (56) Stiehl, J. D.; Kim, T. S.; McClure, S. M.; Mullins, C. B. *J. Am. Chem. Soc.* **2004**, *126*, 1606.
- (57) Ishida, T.; Nagaoka, M.; Akita, T.; Haruta, M. *Chem.—Eur. J.* **2008**, *14*, 8456.
- (58) Lü, G.; Ji, D.; Qian, G.; Qi, Y.; Wang, X.; Suo, J. *Appl. Catal., A* **2005**, *280*, 175.
- (59) Zhu, K.; Hu, J.; Richards, R. *Catal. Lett.* **2005**, *100*, 195.
- (60) Larsen, R. G.; Saladino, A. C.; Hunt, T. A.; Mann, J. E.; Xu, M.; Grassian, V. H.; Larsen, S. C. *J. Catal.* **2001**, *204*, 440.
- (61) Sun, H.; Blatter, F.; Frei, H. *J. Am. Chem. Soc.* **1996**, *118*, 6873.
- (62) Chen, G. Z.; Wu, S. J.; Liu, H. L.; Jiang, H. F.; Li, Y. W. *Green Chem.* **2013**, *15*, 230.